Electron paramagnetic resonance study of Fe^{3+} at M_1 position in forsterite

1997 J. Phys.: Condens. Matter 9 10033

(http://iopscience.iop.org/0953-8984/9/45/029)

J. Phys.: Condens. Matter **9** (1997) 10033–10039. Printed in the UK PII: S0953-8984(97)84249-X

Electron paramagnetic resonance study of Fe^{3+} at M_1 position in forsterite

J-M Gaite† and H Rager‡

† Centre de Recherche sur la Matière Divisée, Université d'Orléans—CNRS, Rue de Chartres, BP 6759, 45067 Orléans Cédex 2, France

‡ Institute of Mineralogie, University of Marburg, Hans Meerwein Strasse, 3550 Marburg, Germany

Received 16 May 1997, in final form 28 July 1997

Abstract. In an electron paramagnetic resonance study of a synthetic single crystal of forsterite, Mg_2SiO_4, one spectrum of Fe^{3+} with maximum local symmetry -1 was observed. This spectrum arises from Fe^{3+} substituted for Mg^{2+} at the M_1 position. The second-order constants of the spectrum are $b_2^0 = 0.184$ cm^{-1} and $b_2^2 = 0.1422$ cm^{-1}. All the fourth-order spin-Hamiltonian constants are given: they are much larger than generally observed in silicates. The zero-field splitting of the EPR spectrum is larger than the energy of the hyperfrequency field in the Q band; this case is near the limit of possibility of calculating the fourth-order constants of the spin Hamiltonian. It is shown that the substitution of Fe^{3+} for Mg^{2+} does not strongly modify the local structure and that there is no local charge compensation.

1. Introduction

Forsterite, Mg_2SiO_4, is an endmember of the solid solution olivine series. It crystallizes with orthorhombic space group *Pnma* and has a relatively dense packing of four formula units per unit cell. The oxygen atoms are approximately hexagonally close packed. Silicon occupies one half of the tetrahedral voids, magnesium one half of the octahedral ones. There are two non-equivalent positions of equal multiplicity for Mg^{2+} ions: M_1 (4a) with point symmetry -1 and M_2 (4c) with point symmetry m. The position for Si is also 4c. Synthetic single crystals several centimetres in size having very good quality may be grown by the Czochralsky method and, hence, doped with small traces of transition ions such as Cr^{3+}, Mn^{2+}, Fe^{3+} or rare earth ions like Gd^{3+}. Recently, rather interesting laser properties of Cr-doped forsterite have been reported (see, e.g. Petricevic *et al* 1989). In several cases, the EPR studies show that the paramagnetic impurities are not equally distributed over the M_1 and M_2 positions: for example, it was observed that Mn^{2+} and Gd^{3+} in low concentration are located only at M_2 (Chatelain and Weeks 1970, Gaite and Michoulier 1973, Gaite 1980).

A detailed EPR study of Fe^{3+} in forsterite has been previously reported. This study describes the EPR spectra of Fe^{3+} at M_1 and Si positions. The studied sample had about 60% of Fe^{3+} at M_1 and 40% at Si positions. Only very low-intensity lines were detected arising from Fe^{3+} at a lower-symmetry position. They were not studied because of their too low intensity (Gaite and Hafner 1984).

The purpose of the present paper is to study the previously detected spectra using another sample.

0953-8984/97/4510033+07$19.50

2. The crystal and the EPR spectra

The crystal used for the present study was previously studied by Chatelain and Weeks (1973) who gave the first description of the EPR spectra of Fe^{3+} substituted for Mg^{2+} at the M_2 position. However, several resonance lines were not explained. Therefore, new EPR measurements on the original crystal specimen of Chatelain and Weeks were performed.

The angular dependence of the transition lines was taken at both X- and Q-band frequencies in the three crystallographic planes. Hence, it was possible to identify different centres. The Q-band EPR spectrum for B parallel to the crystallographic c axis is presented in figure 1. The main characteristics of the various EPR species are the following. Narrow hyperfine lines around 1250 mT are characteristic of Mn^{2+} at M_2 (Gaite and Michoulier (1973)); we also observed very low-intensity lines (not visible in figure 1) belonging to Mn^{2+} at a low-symmetry position. These lines may arise from Mn^{2+} at the M_1 position, but the transitions were masked by other strong lines. Therefore, it was not possible to study this spectrum in detail.

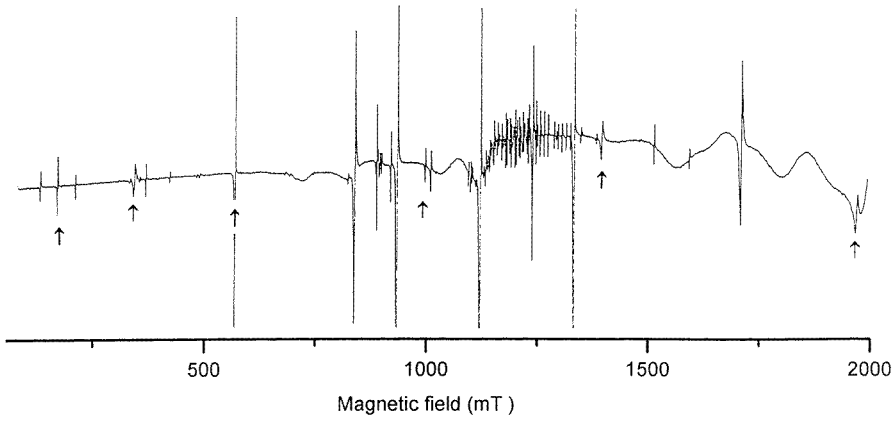

Figure 1. Q-band EPR spectrum at room temperature of the forsterite single crystal. The magnetic field is parallel to the crystallographic c axis. Transition lines indicated by arrows belong to the Fe^{3+} spectrum under investigation.

Further, a spectrum with no characteristic symmetry was observed arising perhaps from iridium (four hyperfine lines near 870 mT). Although such a centre was never observed in forsterite, its presence is not surprising for the sample was grown in an iridium crucible. this spectrum was not studied in detail. All other strong lines of the EPR spectra are related to Fe^{3+}. Among them, we identified an intensive spectrum due to Fe^{3+} at M_2 and also a weak one corresponding to Fe^{3+} substituted for Si^{4+} (Gaite and Hafner 1984). Lines indicated by arrows in figure 1 belong to an Fe^{3+} centre whose symmetry is lower than monoclinic. The Fe^{3+} centre reveals four equivalent subspectra which are related by symmetry and superimpose 2 by 2 in the three crystallographic planes. In the Q band this spectrum (i.e. the number of observed transitions and the line intensities) strongly depends on the orientation of the magnetic field with respect to the crystal axis system. However, enough transitions could be observed to perform a complete evaluation of this new Fe^{3+} spectrum. A first study of this spectrum was done in the X band by Niebuhr (1976). In the X band only the transitions inside the Kramers doublet $|-\frac{3}{2}\rangle - |\frac{3}{2}\rangle$ were observable. The

X-band experiments were used as a first approach to identify the transitions observed in the Q-band spectra whose angular dependence is very unusual and complicated.

3. Characteristics of the new Fe^{3+} spectrum

From the measurements of the transitions for several orientations of the magnetic field lying in the three crystallographic planes, we determined the constants of the general spin Hamiltonian of Fe^{3+} defined by

$$H_4 = \sum_{ij} g_{ij}\beta B_i S_j + \sum_{m=-2}^{2} B_2^{\prime m} O_2^{\prime m} + \sum_{m=-4}^{4} B_4^{\prime m} O_4^{\prime m}.$$

g_{ij} are the components of the Zeeman g matrix, $B_n^{\prime m}$ the fine-structure constants and $O_n^{\prime m}$ ($n = 2, 4$) the normalized Stevens operators. The spin Hamiltonian is more commonly written using the Stevens operators O_n^m and the associated constants b_n^m, although they are not consistently transformed under rotation. To avoid any misunderstanding or confusion about the results, we report in table 1 both $B_n^{\prime m}$ and b_n^m constants.

Table 1. Spin-Hamiltonian parameters of the studied Fe^{3+} spectrum in forsterite expressed in the *abc* crystallographic reference system. All fine structure constants are expressed in 10^{-4} cm^{-1}.

g-matrix elements		Fine-structure constants				
ij	g_{ij}	m	$B_2^{\prime m}$	b_2^m	$60B_4^{\prime m}$	b_4^m
xx	2.0049	0	82.1	82.1	−40.67	−40.67
yy	2.0025	1	1816.7	6293.2	−20.37	−128.83
zz	2.0042	−1	545.9	1891.1	12.54	79.31
xy	0.0003	2	160.4	555.6	44.72	200.00
xz	0.0020	−2	670.5	2322.6	124.32	555.97
yz	−0.0038	3			−1.48	−24.76
		−3			13.14	219.87
		4			−34.30	−202.92
		−4			50.20	296.99

Looking first at the g-matrix components, it is seen that the g tensor is not purely isotropic, the anisotropy being much larger than generally observed for Fe^{3+}.

By the example of the energy diagram presented in figure 2 it can be seen that the zero-field splitting is larger than the microwave energy $h\nu$ (at Q-band frequency: $h\nu \approx 1.2$ cm^{-1}). The splitting between the two lower doublets is 1.67 cm^{-1}, and 2.03 cm^{-1} between the two others. For the particular orientation of the magnetic field used to calculate the energy diagram, six transitions were measured (figure 1) instead of five in the case of low zero-field splitting. That means we have more data than necessary to calculate the spin-Hamiltonian constants, but the number of observed transitions strongly depends on the orientation of the magnetic field with respect to the crystal axis system. This can be easily explained using figure 2. For the particular orientation presented, there are two transitions between the 2 and 3 energy levels and also between the 3 and 4 ones, the energy levels being labelled in increasing order. When the magnetic field is rotated, the dependences of the energy levels on the magnetic field are modified and some transitions may disappear. For some orientations no transitions between the 2 and 3 levels were observed. In the present case enough lines could be measured to calculate precisely all constants. However, with a slightly larger

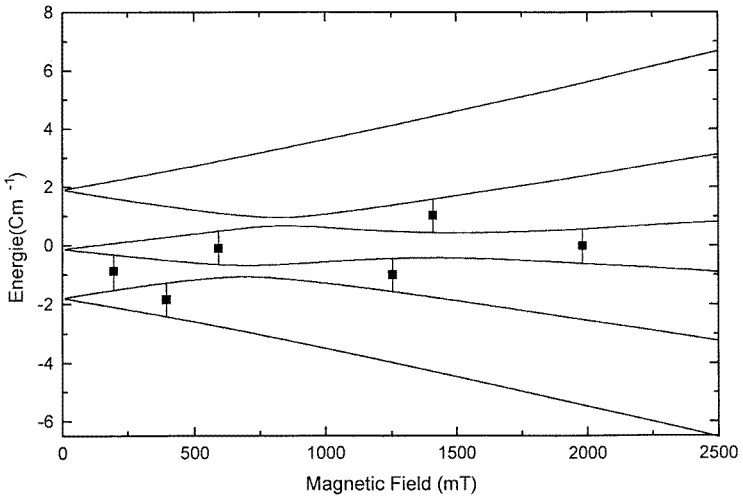

Figure 2. Diagram of the energy levels of Fe^{3+} for B parallel to c. Transitions indicated on the diagram were used for the calculation of the spin-Hamiltonian constants.

Table 2. Orientations of the M_1–O direction of the principal axis of the second-order tensor of Fe^{3+} compared to those of Cr^{3+} at the M_1 position and to the extrema of the angular dependence of the Fe^{3+} spectrum at X-band frequency (EPR axes).

M_1–O_6 octahedron				Second-order tensor: Fe^{3+}		EPR axes: Fe^{3+}		Second-order tensor: Cr^{3+}	
d (nm)	θ	ϕ	axes	θ	ϕ	θ	ϕ	θ	ϕ
0.2091	44.2	39.9	OX	109.6	103.1	114.8	89.2	50.8	38.4
0.2075	136.2	21.8	OY	48.4	174.7	54.5	160.1	59.5	157.0
0.2142	84.5	128.4	OZ	48.0	31.7	45.7	26.0	125.8	87.7
			b_2^0 (cm^{-1})	0.1845				0.433	
			b_2^2 (cm^{-1})	0.1422				0.283	
			$\lambda = b_2^2/b_2^0$	0.77				0.83	

zero-field splitting only transitions inside the Kramers doublets could be observed for most observations, removing the possibility of calculating the fourth-order constants of the Fe^{3+} spectrum. Therefore, the present example indicates the experimental limit for the precise determination of all Fe^{3+} spin-Hamiltonian constants.

From the second-order constants, we determined the eigenvectors of the second-order tensor and its reduced values. The results are presented in table 2 together with the results deduced from the X-band experiment and with the EPR data of Cr^{3+} at the M_1 position (Rager 1977). The orientations of the axes given in table 2 are illustrated in figure 3.

From these results it follows that the eigenvectors of the second-order tensor differ significantly from the EPR axes obtained in the X-band. This can be explained by the large parameter $\lambda = 0.77$. In such a case the angular dependence of the $|-\frac{3}{2}\rangle \rightarrow |\frac{3}{2}\rangle$ transitions, which can only be observed at X-band frequencies, is very small and, additionally, affected by the anisotropy of the g tensor and perhaps by the fourth-order terms. Then, the extrema of the angular dependence (EPR axes) do not coincide with the eigenvectors of the second-

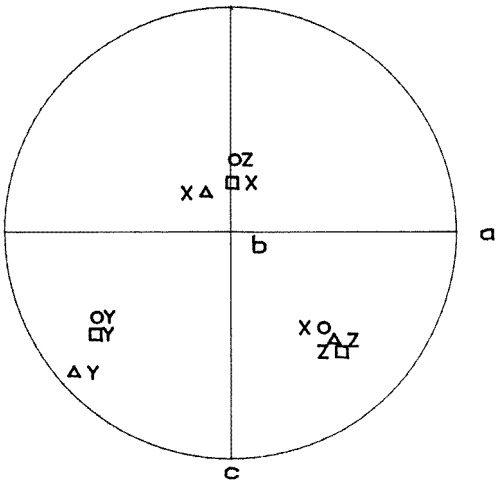

Figure 3. Comparison of the orientation of the axes of the second-order tensors of Fe^{3+} (triangles), Cr^{3+} (circles), and the extrema of the angular dependences of the $|-\frac{3}{2}\rangle \rightarrow |\frac{3}{2}\rangle$ transition determined from X-band experiment (EPR axes) (squares).

rank tensor. The axes of the second-rank tensor are close to those of Cr^{3+} at the M_1 position; it may be supposed that the spectrum under investigation arise from Fe^{3+} at the same position, the crystal field around the paramagnetic ion being the same if there is not to much lattice relaxation induced by the substitutions.

4. Pseudo-symmetries of H_4 and of the M_1–O_6 octahedron

To obtain information on the Fe^{3+} environment, we determined the pseudo-symmetry characteristics of $H_4 = \sum B_4'^m O_4'^m$, following the method proposed by Michoulier and Gaite (1972).

The fourth-order term of the spin Hamiltonian is considered to be mainly induced by the nearest neighbours of Fe^{3+}, and the pseudo-symmetries of H_4 are representative of those of the Fe^{3+} environment.

The pseudo-symmetries of H_4 are characterized by the orientations (θ, ϕ) with respect to the initial reference frame of the n-fold (fourfold and threefold) pseudo-symmetry axes and by ε_n parameters.

The ε_n parameters are defined by

$$\varepsilon_n = \left[((B_4'^0)^2 + (B_4'^n)^2 + (B_4'^{-n})^2) \left(\sum (B_4'^m)^2 \right)^{-1} \right]_{min(\theta,\phi)} \qquad \text{for } n = 3 \text{ and } 4.$$

The ε_n are zero in the case of perfect symmetry and their values are characteristic of the distortion of the environment of the studied ions.

We also determined the distortion of H_4 from cubic symmetry. H_4 is written as the sum of a cubic term H_{4c} and a distortion part H_{4d}. H_{4c} is expressed in a reference system whose polar axis is along a fourfold symmetry axis; it is described by a constant a' equal to the usual cubic constant a in the case of real cubic symmetry.

The expression of a' is given by

$$a' = 70(|B_4'^0| + (5/7)^{1/2}((B_4'^4)^2 + (B_4'^{-4})^2)^{1/2})_{max(\theta,\phi)}.$$

In a systematic study of a' as a function of the angles θ and ϕ, since a maximum is reached the orientation of one fourfold axis of H_{4c} is obtained.

The distortion from cubic symmetry is defined by the parameter $d = (a^{*2} - a'^2)/a^{*2}$: a^* is defined by $a^* = 120[(7/12)\sum(B_4'^m)^2]$.

The basis of this procedure was established by Gaite (1975, 1987), and more complete applications are given by Gaite *et al* (1991).

All results are reported in table 3. The orientations of the axes obtained by the two independent methods agree within 0.2°, and, therefore, only the orientations of the axes obtained by the first method are given.

Table 3. Characteristics of the pseudo-symmetries of the fourth-order term of the spin Hamiltonian of Fe^{3+}, compared to those of the M_1–O_6 octahedron obtained from crystal field calculations and by a geometrical model.

	Fe^{3+} at M_1			Crystal field at M_1			Geometric model		
n	100ε	θ	ϕ	100ε	θ	ϕ	100ε	θ	ϕ
4	4.24	136.8	31.8	2.57	135.5	32.1	1.37	135.5	33.3
4	3.19	46.8	33.8	1.96	45.5	36.7	1.38	45.6	36.4
4	2.99	90.6	123.1	1.94	92.5	124.2	1.37	91.5	124.9
3	2.37	146.0	126.0	1.84	147.1	125.5	0.88	146.1	125.3
3	4.07	91.9	68.1	2.18	91.6	69.7	1.08	91.7	70.1
3	3.26	36.2	120.3	1.63	37.3	123.2	0.46	37.1	124.3
3	3.64	89.4	177.5	2.29	90.9	179.2	1.29	90.3	179.5
$a^*/2$	117.2×10^{-4} cm^{-1}								
$a'/2$	114.7×10^{-4} cm^{-1}								
d	0.042								

To characterize the M_1–O_6 octahedron, we used the crystallographic data given by Birle *et al* (1968). From these data, we computed the constants of the fourth-order development of the crystal field at M_1 position in terms of Tesseral harmonics as described by Hutchings (1964), and used the same procedure than for H_4. We also determined the pseudo-symmetries of the non-substituted M_1–O_6 octahedron using the geometrical model proposed by Gaite (1980). All these results are given in table 3.

It was said previously that the orientations of the pseudosymmetry axes of H_4 obtained using the two independent methods are very close. This is not surprising since the distortion d, although it is four times larger than for Fe^{3+} at the M_2 position, is quite small ($d = 0.11$ for Fe^{3+} substituted for Si^{4+} in forsterite).

Looking at the values of the ε_n parameters for H_4, all of them are of the same order of magnitude: this means that the environments of Fe^{3+} do not have a simple axial distortion. The comparison of the orientations of the pseudo-symmetry axes of H_4 to those of the M_1 site determined in the two different ways shows clearly that there is a very good fitting between all of them. In addition to this, we can remark that for the M_1 site there is no simple characteristic axial distortion as was deduced from the values of H_4.

Then it can be deduced that Fe^{3+} at the M_1 position is responsible for the present EPR spectra and that there is no charge compensation in the first coordination shell.

5. Discussion

Looking at the forsterite structure the orientations of the M–O directions for the M_1 and M_2 octahedra are not very far from one another, and subsequently the orientations of the pseudosymmetry axes of the fourth-order term of the development of the crystal field are close (for example M_2, ($\theta = 90.0$, $\phi = 123$; M_1, $\theta = 92.5$, $\phi = 124.2$). Then for the new spectrum we studied it could be considered that Fe^{3+} may be located at M_2, but that the presence of a charge compensator could be responsible for the local symmetry lowering. Several arguments are against this hypothesis. The second-order constants of Fe^{3+} at M_2 are far from those determined in the present study, so the compensator should be close to the Fe^{3+} at M_2: as a consequence a pronounced axial pseudo-symmetry should be observed from H_4. Moreover, the orientations of the second-order term are close to those of Cr^{3+} at M_1. On the other hand the presence of a charge compensator in the second coordinating shell would not produce such an important change of all the spin-Hamiltonian constants.

One point can be mentioned here. In the crystal we studied, only a small amount of the total Fe^{3+} was at the Si position, and the distribution of Fe^{3+} at M_1 and M_2 was estimated from the X-band experiment to be 70% at M_2 and 30% at M_1 (Nieburgh 1976) whereas in the crystal studied by Gaite and Hafner (1984), grown by the same method, Fe^{3+} was distributed mainly at the M_2 position (60%) and silicon position (40%). Such a large difference in the Fe^{3+} distribution is surely due to differences in the preparation of the samples, but they are not known.

Looking now at the fourth-order constants we must first remark that the norm of this term or the related constant a^* is much bigger than that generally observed for Fe^{3+} in oxygen octahedral environments in silicates. The value of $a^*/2$ for Fe^{3+} at the M_2 position is only 40.6×10^{-4} cm^{-1}, while in the present case the calculated value (117.2×10^{-4} cm^{-1}) is three times bigger. Since the fourth-order term is mainly induced by the nearest neighbours, there is surely a very strong interaction between Fe^{3+} and the oxygen ligands in the present case.

References

Birle J D, Gibbs P B, Moore P B and Smith J V 1968 *Am. Mineral.* **53** 807

Chatelain A and Weeks R A 1970 *J. Chem. Phys.* **52** 5682

——1973 *J. Chem. Phys.* **58** 3722

Gaite J-M 1975 *J. Phys. C: Solid State Phys.* **8** 3887

——1980 *Phys. Chem. Miner.* **6** 9

——1987 *Electron Magnetic Resonance of the Solid State* ed J A Weil (Ottawa: The Canadian Society for Chemistry) p 151

Gaite J-M and Hafner S S 1984 *J. Chem. Phys.* **80** 2747

Gaite J-M and Michoulier J 1973 *Proc. 17th Congress Ampere (Turku, 1973)*

Gaite J-M, Stenger J F, Dusausoy Y, Rager H and Marnier G 1991 *J. Phys.: Condens. Matter* **3** 7877

Hutchings M T 1964 *Solid State Physics* vol 16 (New York: Academic) p 227

Michoulier J and Gaite J-M 1972 *J. Chem. Phys.* **56** 5205

Niebuhr H 1976 *Habilitation Thesis* Philipps-Universität Marburg

Petricevic V, Gayen S K and Alfano R R 1989 *OSA Proc. Tunable Solid State Lasers* vol 5, ed M L Shand and H P Jenssen (Woodbury, NY: Optical Society of America) p 77

Rager H 1977 *Phys. Chem. Miner.* **1** 371